

# Ultradense Dark Matter Halos with Poisson Noise from Stellar-Mass Primordial Black Holes

Saeed Fakhry<sup>1,2,\*</sup>

<sup>1</sup>*Department of Physics, Shahid Beheshti University, 1983969411, Tehran, Iran*

<sup>2</sup>*PDAT Laboratory, Department of Physics, K.N. Toosi University of Technology, P.O. Box 15875-4416, Tehran, Iran*

(Dated: February 4, 2025)

In this study, we investigate the effect of Poisson noise, originating from the discrete distribution of stellar-mass primordial black holes (PBHs), on the abundance of ultradense dark matter halos (UDMHs). We incorporate the contribution of PBH shot noise into the power spectrum and modify the primordial power spectrum to calculate the differential mass function of UDMHs across various models, while accounting for crucial physical and geometrical factors. We further compare our results with observational constraints on the abundance of compact dark matter and the mass distribution of PBHs derived from the thermal history of the early Universe. Our findings demonstrate that the mass of PBHs contributing to Poisson noise plays a pivotal role in determining the abundance of UDMHs. Moreover, we show that Poisson noise from lighter PBHs strengthens the single-component dark matter scenario, whereas the corresponding effect from heavier PBHs supports multi-component dark matter scenario.

## I. INTRODUCTION

The hierarchical nature of cosmic structure formation is characterized by a bottom-up evolutionary path, in which gravitationally bound objects emerge from the collapse of random density perturbations and subsequently undergo hierarchical mergers [1–5]. While this process is largely driven by the initial perturbations of moderate amplitude inflation ( $\delta \sim 10^{-5}$ ), there may be some theoretical frameworks that can predict deviations from this conventional paradigm, see, e.g., [6–12]. In this regard, primordial black holes (PBHs) are strong candidates for macroscopic dark matter that may have formed from large-amplitude ( $\delta \gtrsim 0.3$ ) primordial density fluctuations in the early Universe, see, e.g., [13–16]. PBHs can explain various astrophysical phenomena, notably the gravitational wave signals generated by merging black hole binaries detected by the LIGO-Virgo-Kagra collaboration [17, 18], if they act as entire or a fraction of dark matter content [19–27].

An essential but often overlooked component of PBH-dominated dark matter scenarios is the intrinsic Poisson statistics that dictate their discontinuous distribution [28]. The formation of PBHs induces entropy perturbations that appear in the matter power spectrum and give rise to a Poisson spatial distribution [29]. This feature significantly distinguishes PBH models from particle dark matter frameworks, where the matter distribution is usually approximated as a continuous fluid [30]. The inherent discreteness of PBH distributions introduces significant shot noise, which substantially alters the matter power spectrum at small scales and, consequently, the dynamics of the formation of compact dark matter structures [31]. These Poisson fluctuations affect not only the direct distribution of PBHs, but also the formation of other dark matter structures, especially in moderate-amplitude overdensities. The magnitude of this shot noise contribution scales inversely with the number density of PBHs, making it particularly relevant for scenarios involving massive PBHs where their spatial

number density is naturally lower [32].

Furthermore, in contrast to conventional cold dark matter predictions, Poisson fluctuations may accelerate the growth of cosmic structures in the early Universe by inducing early structure formation. In regions where the characteristic scale of the shot noise approaches that of the primordial disturbances, the interaction between Poisson noise and the underlying density field becomes particularly complex, resulting in non-trivial modifications of the normal structure development paradigm [33]. Given that next-generation surveys investigating the high-redshift Universe may soon verify these predictions, it is imperative to comprehend these alterations in order to make accurate predictions about the quantity and characteristics of early cosmic structures in PBH scenarios [34, 35].

Although PBHs emerge from substantial density fluctuations, more moderate overdensities ( $\delta \gtrsim 10^{-3}$ ) can facilitate the formation of ultradense dark matter halos (UDMHs) [36–39]. These structures, while lacking an event horizon, exhibit greater sensitivity to small-scale perturbations, thereby acting as sensitive probes of the initial small-scale power spectrum [40]. The formation of dark matter halos has been investigated using both numerical simulations and analytical methods, with a particular focus on those that emerged during the matter-dominated era, see, e.g., [41–45]. Numerous studies have been conducted to specifically explore the formation of UDMHs during the radiation-dominated era, see [46–50]. The mass scale of UDMHs is intrinsically linked to the horizon mass at the time fluctuations re-enter the cosmological horizon. Smaller-scale perturbations, which re-enter earlier, experience extended periods of overdensity growth, enhancing their development. The interplay between Poisson-induced fluctuations and these moderate-density regions can establish distinct conditions for UDMH formation, setting them apart from conventional structure formation processes.

In this study, we introduce a modified matter power spectrum that incorporates the influence of Poisson noise arising from stellar-mass PBHs and examine its implications for the formation of UDMHs. The paper is structured as follows: In Section II, we analyze the formation and evolution of UDMHs during the radiation-dominated epoch. Additionally, we characterize their abundance using more realistic mass functions

\* [s.fakhry@sbu.ac.ir](mailto:s.fakhry@sbu.ac.ir)

and a refined power spectrum that accounts for Poisson noise contributions from stellar-mass PBHs. In Section III, we present our results and provide a detailed discussion on the abundance of UDMHs. Finally, in Section IV, we summarize the key conclusions of our investigation.

## II. FORMATION OF UDMHS

The evolution of linear density perturbations in dark matter during the radiation-dominated era, initiated by primordial curvature perturbations  $\zeta$ , is characterized by:

$$\begin{aligned}\delta(k, a) &= \alpha \zeta(k) \log \left( \beta \frac{a}{a_{\text{H}}} \right) \\ &= \alpha \zeta(k) \log \left( \sqrt{2} \beta \frac{k}{k_{\text{eq}}} \frac{a}{a_{\text{eq}}} \right),\end{aligned}\quad (1)$$

where  $a \gg a_{\text{H}}$ , with  $a_{\text{H}}$  being the scale factor at horizon entry. The parameters  $k_{\text{eq}} \simeq 0.01 \text{ Mpc}^{-1}$  and  $a_{\text{eq}} \simeq 3 \times 10^{-4}$  represent the horizon scale and scale factor at matter-radiation equality, respectively. Numerical estimates suggest  $\alpha = 6.4$  and  $\beta = 0.47$  [51]. Additionally, the scale factor at horizon crossing is given by:

$$\frac{a_{\text{H}}}{a_{\text{eq}}} = \frac{1 + \sqrt{1 + 8(k/k_{\text{eq}})^2}}{4(k/k_{\text{eq}})^2} \simeq \frac{\sqrt{2}}{2} \frac{k_{\text{eq}}}{k}, \quad k \gg k_{\text{eq}}. \quad (2)$$

Non-relativistic dark matter is thought to have been disconnected from radiation during the horizon crossing. Individual dark matter particles' motion, driven by curvature perturbations, can be described as an ellipsoid's axis drifting independently. The initial tidal field of an area with scale  $k$  dictates its eccentricity  $e$  and prolateness  $p$ , which in turn influence the axis ratios of the ellipsoidal drift. The density evolution in such an area depends on the contraction or expansion of each axis caused by particle motion, as defined by:

$$\frac{\rho}{\bar{\rho}_{\text{m}}} = \prod_{i=1}^3 |1 - \lambda_i \delta(k, a)|^{-1}, \quad (3)$$

where  $\bar{\rho}_{\text{m}}$  denotes the mean dark matter density, and  $\lambda_i$  are the eigenvalues of the deformation tensor under the Zeldovich approximation:

$$\lambda_1 = \frac{1 + 3e + p}{3}, \quad \lambda_2 = \frac{1 - 2p}{3}, \quad \lambda_3 = \frac{1 - 3e + p}{3}. \quad (4)$$

Collapse along a given axis  $i$  occurs when the linear density perturbation  $\delta(k, a)$  exceeds  $\lambda_i^{-1}$ . The axis associated with the smallest eigenvalue ( $\lambda_3$ ) collapses last, and the entire ellipsoidal region collapses when  $\lambda_3 \delta(k, a_c) = 1$ , where  $a_c$  denotes the collapse scale factor. The critical density contrast under these conditions is given by:

$$\delta_{\text{c}} = \frac{3}{1 - 3e + p}. \quad (5)$$

The most likely values for  $e$  and  $p$  are  $e_{\text{mp}} = \sigma/(\sqrt{5}\delta)$  and  $p_{\text{mp}} = 0$ , respectively, given a Gaussian random field with

density contrast  $\delta$  and linear root-mean-square  $\sigma$  [52]. According to the excursion set formalism, the moving barrier is  $B(S) = 3(1 + \sqrt{S/5})$ , with  $S \equiv \sigma^2$ . These values result in a collapse threshold of  $\delta_{\text{c}} = 3(1 + \sigma/\sqrt{5})$  [53]. Therefore, collapse can happen during the radiation-dominated epoch if the density perturbations are high enough. Only the rarest spikes can produce PBHs, although moderate perturbations can make UDMHs.

It is crucial to note that halos did not always form from collapsing structures during the radiation-dominated era. Numerical simulations show that a collapsed peak only creates a virialized halo when it changes to a locally matter-dominated state [54]. In contrast, collapsed regions are substantially denser than the surrounding dark matter, with their densities scaling as  $\sim e^{-2} \bar{\rho}_{\text{m}}$  [38]. Given the typical ellipticity  $e \sim 0.15$  of the tidal field at a  $3\sigma$  peak, local matter dominance occurs at  $a/a_{\text{eq}} \sim e^2 \simeq \mathcal{O}(10^{-2})$ . As a result, halos form long before matter dominion begins. The density within these halos is quite high, as they scale with the average cosmic density at the time of formation

### II.1. Halo mass functions

The unconditional halo mass function, which characterizes the average comoving number density of halos inside a logarithmic mass interval, is provided by the excursion set theory [53].

$$\frac{dn}{d \log M} = \frac{\bar{\rho}_{\text{m},0}}{M} \left| \frac{d \log \nu}{d \log M} \right| \nu f(\nu). \quad (6)$$

In this case, the comoving average density of dark matter content is represented as  $\bar{\rho}_{\text{m},0} \simeq 33 \text{ M}_{\odot}/\text{kpc}^3$ , and the dimensionless parameter  $\nu \equiv \delta_{\text{c}}/\sigma$  is referred to as peak height. Additionally, the distribution of first crossings is represented by the function  $f(\nu)$ , also referred to as the "multiplicity function." The root-mean-square of linear density fluctuations smoothed on the mass scale  $M$  is represented by:

$$\sigma^2(M, a) = \frac{1}{2\pi^2} \int_0^{\infty} P(k, a) W^2(k, M) k^2 dk, \quad (7)$$

where  $W(k, M)$  is the smoothing window function, which is considered to be a sharp- $k$  filter, and  $P(k, a)$  is the power spectrum of linear matter fluctuations [53],

$$W(k, M) = \begin{cases} 1 & \text{if } 0 < k \leq k_M \\ 0 & \text{otherwise} \end{cases} \quad (8)$$

with  $k_M = (6\pi^2 \bar{\rho}_{\text{m},0}/M)^{1/3}$  [55]. In these situations, one can have

$$\frac{d \log \nu}{d \log M} = \frac{k_M^3}{12\pi^2} \frac{P(k_M, a)}{\sigma^2(M, a)}. \quad (9)$$

From Eq. (1), it follows that

$$P(k, a) = \frac{2\pi^2 \alpha^2}{k^3} \left[ \log \left( \sqrt{2} \beta \frac{k}{k_{\text{eq}}} \frac{a}{a_{\text{eq}}} \right) \right]^2 P_{\zeta}(k), \quad (10)$$

where  $P_\zeta(k)$  represents the dimensionless power spectrum of primordial curvature perturbations. The exact shape of  $P_\zeta(k)$  depends on the hypothesized inflationary scenario that causes the perturbations. In the next section, we propose modifying the power spectrum to account for the Poisson noise of stellar-mass PBHs at small scales.

This study aims to investigate how physical elements affect the halo mass function in the ultradense domain of excursion set theory, specifically their impact on the dynamical barrier. To determine the distribution of initial crossings in scenarios with various barriers, simulate a large number of random walks. [56, 57]. According to [57], for various dynamical barriers, the initial crossing distribution can be approximated by

$$f(S) = |T(S)| \exp\left(-\frac{B(S)^2}{2S}\right) \frac{1}{S\sqrt{2\pi S}}, \quad (11)$$

where  $T(S)$  is given by the Taylor expansion of  $B(S)$

$$T(S) = \sum_{n=0}^5 \frac{(-S)^n}{n!} \frac{\partial^n B}{\partial S^n}. \quad (12)$$

[38] derive an approximation for the distribution of first barrier crossings within a Gaussian random walk framework, validated by Monte Carlo simulation,

$$f(S) \approx \frac{3 + 0.556\sqrt{S}}{\sqrt{2\pi S^3}} \exp\left(-\frac{B^2}{2S}\right) \left(1 + \frac{S}{400}\right)^{-0.15}, \quad (13)$$

which corresponds to the PS multiplicity function<sup>1</sup>,

$$[\nu f(\nu)]_{\text{PS}} = \sqrt{\frac{2}{\pi}} \frac{(\nu + 0.556) \exp[-0.5(1 + \nu^{1.34})^2]}{(1 + 0.0225\nu^{-2})^{0.15}}. \quad (14)$$

It should be noted that discrepancies exist between the predictions of the PS mass function and the distribution of dark matter halos, particularly at high redshifts [59]. These discrepancies, as previously noted, may arise from various physical factors overlooked in the PS formalism, which could significantly influence the abundance of UDMHs. One key factor addressed here involves geometry, extending the spherical-collapse model foundational to the PS formalism to ellipsoidal-collapse halo models. This modification leads to the Sheth-Tormen (ST) mass function, as outlined by [52]

$$[\nu f(\nu)]_{\text{ST}} = A_1 \sqrt{\frac{2\nu'}{\pi}} \left(1 + \frac{1}{\nu'^q}\right) \exp\left(-\frac{\nu'}{2}\right), \quad (15)$$

where  $q = 0.3$ ,  $\nu' \equiv 0.707\nu^2$ , and  $A_1 = 0.322$  determined by ensuring that the integral of  $f(\nu)$  over all possible values of  $\nu$  equals unity.

<sup>1</sup> The statement explains how the multiplicity function  $f(\nu)$  is connected to the first crossing distribution  $f(S, t)$ . The latter represents the probability distribution for the first time a random walk crosses a specific barrier  $B(S)$ . The equation  $\nu f(\nu) = Sf(S, t)$  demonstrates that  $f(\nu)$  can be derived from  $f(S, t)$ , illustrating a fundamental relation within the excursion set theory [58].

In addition to the geometric parameters affecting the virialization of dark matter halos, certain physical factors also substantially influence the collapse of overdense regions and, as a result, the halo mass function. Including these critical physical factors in the analysis is essential, as they encapsulate the fundamental physics driving halo collapse and growth, as well as the mechanisms underlying the formation and evolution of cosmic structures over time. This methodology enables the collapse threshold to dynamically depend on effective physical parameters. Consequently, the barrier adapts to these variables, yielding a more accurate model for halo collapse. Key considerations in these corrections include the effects of angular momentum, dynamical friction, and the cosmological constant on the halo mass function. These adjustments help mitigate discrepancies, particularly in contested mass ranges. Incorporating angular momentum and the cosmological constant yields a revised mass function, known as DP1 in this analysis [60]

$$[\nu f(\nu)]_{\text{DP1}} \approx A_2 \sqrt{\frac{\nu'}{2\pi}} k(\nu') \exp\{-0.4019\nu' l(\nu')\}, \quad (16)$$

with  $A_2 = 0.974$  established through normalization, and

$$k(\nu') = \left(1 + \frac{0.1218}{(\nu')^{0.585}} + \frac{0.0079}{(\nu')^{0.4}}\right), \quad (17)$$

and

$$l(\nu') = \left(1 + \frac{0.5526}{(\nu')^{0.585}} + \frac{0.02}{(\nu')^{0.4}}\right)^2. \quad (18)$$

The impact of dynamical friction on the barrier was also examined in [59], resulting in the mass function referred to as DP2 hereafter

$$[\nu f(\nu)]_{\text{DP2}} \approx A_3 \sqrt{\frac{\nu'}{2\pi}} m(\nu') \exp\{-0.305\nu'^{2.12} n(\nu')\}, \quad (19)$$

where  $A_3 = 0.937$  is determined through normalization, and we obtain

$$m(\nu') = \left(1 + \frac{0.1218}{(\nu')^{0.585}} + \frac{0.0079}{(\nu')^{0.4}} + \frac{0.1}{(\nu')^{0.45}}\right), \quad (20)$$

and

$$n(\nu') = \left(1 + \frac{0.5526}{(\nu')^{0.585}} + \frac{0.02}{(\nu')^{0.4}} + \frac{0.07}{(\nu')^{0.45}}\right)^2. \quad (21)$$

In Section III, we will employ these mass functions to compute the abundance of UDMHs for the modified power spectrum while incorporating Poisson noise contributions from stellar-mass PBHs.

## II.2. Modified power spectrum

The formation of PBHs and UDMHs in the radiation-dominated era demands a significant amplification, approximately  $\mathcal{O}(10^7)$ , of the primordial power spectrum at small

scales, which contrasts with the nearly scale-invariant spectrum observed at larger scales. Hence, it becomes imperative to refine the scale-invariant power spectrum through the incorporation of large-amplitude small-scale fluctuations, as such modifications can enhance the probability of PBH formation.

We analyze the formation of PBHs as a consequence of a phase transition occurring at a critical temperature  $T_c$  within the radiation-dominated era [61]. The emergence of PBHs is hypothesized to result from quantum fluctuations or phase transitions in the early Universe, which induce the collapse of overdense regions into black holes. In this context, deviations from scale invariance, particularly through enhanced small-scale fluctuations, can significantly impact the abundance and mass distribution of PBHs. Under the assumption that accretion following formation is negligible, the black hole mass is considered to be approximately  $M_{\text{PBH}}$ . In this regard, the energy density associated with PBHs can be specified as

$$\rho_{\text{PBH}} = M_{\text{PBH}} n_{0,\text{PBH}} (1 + \delta_p) \left( \frac{T}{T_c} \right)^3, \quad (22)$$

where  $n_{0,\text{PBH}}$  denotes the initial number density of PBHs,  $\delta_p$  represents Poisson fluctuations inherent in their distribution, and the factor  $(T/T_c)^3$  accounts for the dilution in PBH density due to cosmic expansion. Since PBHs do not exhibit correlations on scales larger than the Hubble horizon, the corresponding power spectrum is given by [28]:

$$P_p = \langle |\delta_p(k)|^2 \rangle = n_{0,\text{PBH}}^{-1}. \quad (23)$$

In the limit of small-scale perturbations, i.e.,  $k \gg k_{\text{eq}}$ , the isocurvature transfer function can be approximated as:

$$T_{\text{iso}}(k) = \frac{3}{2} a_{\text{eq}}^{-1}. \quad (24)$$

which is independent of  $k$  [28]. Under such assumptions, the power spectrum of primordial curvature perturbations can be determined as:

$$P_\zeta(k) = P_{\text{ad}}(k) + P_{\text{iso}}(k), \quad (25)$$

where  $P_{\text{ad}}(k)$  represents the adiabatic power spectrum generated by inflation (or another approach to producing scale-invariant adiabatic perturbations):

$$P_{\text{ad}}(k) = A_s \left( \frac{k}{k_s} \right)^{n_s - 1}. \quad (26)$$

Here  $k_s = 5 \times 10^{-2} \text{Mpc}^{-1}$  is the scalar pivot scale and  $A_s = 2.1 \times 10^{-9}$  and  $n_s = 0.96$  are set from cosmic microwave background observations [62]. Moreover,  $P_{\text{iso}}(k)$  is the contribution of Poisson noise from PBHs, which can be defined as

$$P_{\text{iso}}(k) = Q(k) D(k, k_1, w) \exp \left[ \frac{-(k - k_2)^2}{2\sigma^2} \right]. \quad (27)$$

In the above relation

$$Q(k) = T_{\text{iso}}^2(k) P_p \simeq \frac{9M_{\text{PBH}}}{4\rho_{\text{PBH}} a_{\text{eq}}^2}, \quad (28)$$

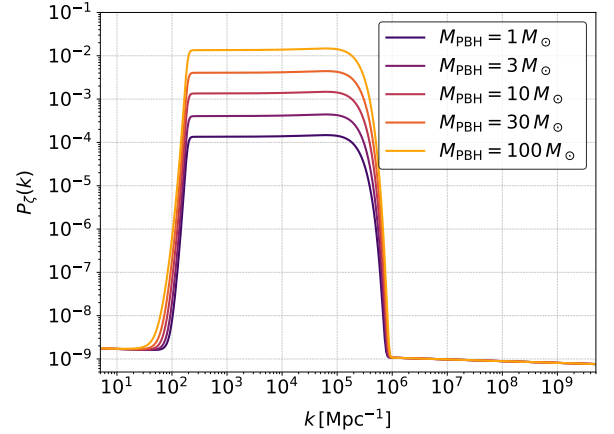


FIG. 1. Modified matter power spectrum as a function of wavenumber  $k$ , described by Eq. (25), while incorporating the impact of Poisson noise from stellar-mass PBHs in the mass range of  $M_{\text{PBH}} = (1-100)M_\odot$ .

and

$$D(k, k_1, w) = \frac{1}{2} \left[ 1 + \tanh \left( \frac{k - k_1}{w} \right) \right], \quad (29)$$

which acts as a smoothing function, where the transition scale is given by  $k_1 \simeq 190 \text{Mpc}^{-1}$  and the width is set to  $w = 15 \text{Mpc}^{-1}$ . Furthermore, a Gaussian function is employed to suppress amplified fluctuations on extremely small scales beyond the cut-off wavenumber  $k_2 \simeq 6 \times 10^4 \text{Mpc}^{-1}$ , with a characteristic width of  $\sigma = 2 \times 10^5 \text{Mpc}^{-1}$ . Consequently, the maximum mass of UDMHs seeded by this power spectrum is naturally constrained to approximately  $10^5 M_\odot$ . In this study, we focus on the Poisson noise from stellar PBHs. Consequently, the mass range of PBHs is chosen to span  $M_{\text{PBH}} = (1-100)M_\odot$ .

In Fig. 1, we have plotted the modified matter power spectrum as a function of wavenumber  $k$ , illustrating the impact of Poisson noise from stellar-mass PBHs across different mass ranges. The curves reveal a distinct enhancement at small scales due to Poisson fluctuations, with more massive PBHs inducing stronger modifications as a result of their lower number density and consequently larger Poisson noise contributions. A key insight is that the Poisson noise contribution can naturally amplify the power spectrum, driven exclusively by the mass characteristics of PBHs. The presence of a plateau in the power spectrum at small scales establishes a fundamental lower bound on large-scale structure formation and serves as a potential observational signature of PBHs as a dark matter candidate. Additionally, the suppression of small-scale structures due to Poisson noise has implications for cosmic structure formation, potentially influencing galaxy clustering and cosmic microwave background anisotropies.

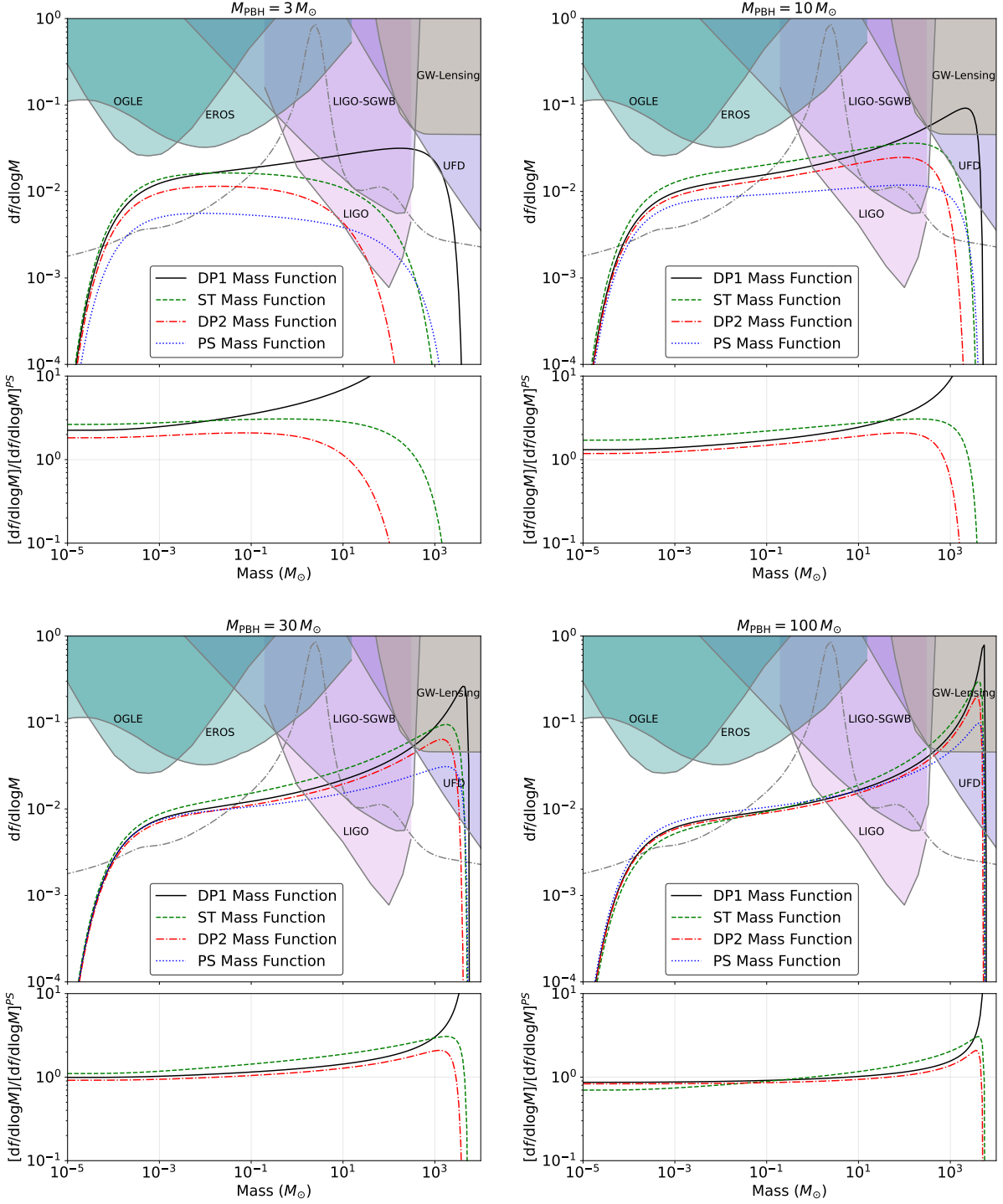


FIG. 2. The differential dark matter mass fraction in UDMHs is presented as a function of mass  $M$ , considering the modified power spectrum from Eq. (25), including Poisson noise from PBHs with masses of  $M_{\text{PBH}} = 3, 10, 30,$  and  $100 M_{\odot}$ . The results for different mass functions are illustrated using various line styles: black solid for DP1, green dashed for ST, red dot-dashed for DP2, and blue dotted for PS at  $a = a_{\text{eq}}$ . Additionally, the gray dot-dashed line represents the PBH mass spectrum derived from the thermal history of the early Universe for  $f_{\text{PBH}} = 1$  [63]. The upper limits from observational constraints on PBHs are included. These constraints are based on microlensing data from EROS [64], the disruption of ultra-faint dwarf galaxies (UFD) [65], gravitational wave microlensing by PBHs (GW-Lensing) [66], microlensing observations from OGLE [67], the stochastic background of PBH mergers detected by LIGO (LIGO-SGWB) [68], and direct constraints on PBH mergers from LIGO observations [69, 70]. The relative deviations of the ST, DP1, and DP2 mass functions compared to the PS mass function are depicted at the bottom of each subfigure.

### III. RRESULTS AND DISCUSSION

In this section, we analyze and compare the predicted abundance of UDMHs by incorporating modifications to halo formation processes, taking into account more realistic mass functions and the influence of Poisson noise from stellar-mass PBHs. Specifically, in Fig. 2, we have computed the differential mass fraction,  $df/d \log M = (M/\bar{\rho}_{m,0})(dn/d \log M)$ , of UDMHs as a function of mass  $M$  at the end of the radiation-dominated era, i.e., at  $a = a_{\text{eq}}$ . We have taken into account three different halo mass functions: the ST approximation, along with the DP1 and DP2 formulations, and compared with the results obtained from the PS formalism. Also, we have considered the impact of Poisson noise by including four distinct PBH masses as  $M_{\text{PBH}} = 3, 10, 30$  and  $100M_{\odot}$ . Furthermore, to facilitate a more precise comparison, we have plotted the three employed mass functions, normalized to the PS mass function, as a function of mass  $M$ .

As can be seen, the impact of Poisson noise becomes more pronounced as PBH mass increases, revealing the complex interactions between noise-induced fluctuations and underlying density fields. This observation challenges conventional paradigms of structure formation, particularly in regions where the characteristic scale of Poisson noise approaches that of primordial disturbances. As the PBH mass increases from 3 to  $100M_{\odot}$ , the differential mass fraction undergoes more substantial modifications, with larger PBH masses inducing stronger Poisson noise due to their lower number densities. This results in more significant alterations in the predicted UDMH abundance across different mass function models.

The mass functions of DP1, ST, and DP2 predict a greater number of high-mass UDMHs ( $M \geq 10^3 M_{\odot}$ ) compared to the PS mass function, with DP1 forecasting the highest abundance for these halos. This highlights the influence of angular momentum corrections, which are the primary physical factor in the DP1 model, as the cosmological constant is not expected to have a significant impact in the early Universe. On the other hand, including dynamical friction decreases the formation of these dense halos, as shown by the DP2 curve. The ST mass function, which incorporates triaxial collapse in the halo formation process, appears to strike a balance and lies between the two previous models. Notably, the predictions derived from various mass functions regarding the abundance of UDMHs exhibit a reasonable level of agreement with the findings presented in [39]. This is despite the fact that the methodology employed in this study to amplify the power spectrum is based on the Poisson noise effect associated with the stellar-mass PBHs, which differs from the approach utilized in the mentioned study.

To analyze the relative abundance of UDMHs and the associated PBHs, we have considered two distinct scenarios. The single-component (SC) scenario assumes that dark matter consists entirely of PBHs, represented by  $f_{\text{PBH}} = 1$ . In contrast, the multi-component (MC) scenario accounts for dark matter as a mixture of PBHs and other components, with  $f_{\text{PBH}} < 1$ .

In the SC scenario, the PBH mass spectrum is determined

based on assumptions regarding the thermal history of the early Universe [63]. Here, the majority of dark matter is composed of PBHs with masses on the order of  $O(1)M_{\odot}$ , while a smaller fraction consists of significantly larger PBHs that act as seeds for the formation of supermassive black holes at galactic centers. A comparison of these scenarios suggests that for masses exceeding  $10M_{\odot}$ , a substantial fraction of dark matter could be in the form of UDMHs, which emerge from the DP1, ST, DP2, and PS mass functions. This suggests that in the SC scenario, UDMH formation likely results from the clustering of smaller PBHs. Conversely, in the MC scenario, UDMHs are expected to form through the virialization of dark matter particles, whereas PBHs arise from the direct collapse of density fluctuations. To assess the abundance of UDMHs relative to PBHs, we compare our results with observational constraints on PBH abundance for extended mass functions [71]. These constraints include microlensing limits from EROS and OGLE [64, 67], direct PBH merger constraints from the LIGO detector [69, 70], the stochastic background of PBH mergers observed by LIGO [68], microlensing of gravitational waves by PBHs [66], and constraints from the disruption of ultra-faint dwarf galaxies (UFDs) [65].

The findings indicate that UDMHs in this scenario are expected to have a significant abundance, particularly in the high-mass region of the mass spectrum, even within parameter spaces already excluded by observational data. Furthermore, a higher number of UDMHs is expected to form during the radiation-dominated era compared to PBHs, as noted in [37, 72]. Additionally, all halo formation models predict a mass function peak around  $M \simeq 10^5 M_{\odot}$ , constrained by the transition scale  $k = 190 \text{ Mpc}^{-1}$ . Among these, the DP1 mass function exhibits the highest peak, exceeding the PS prediction by several factors. The sharp decline in the low-mass tail of the mass functions can be attributed to the large- $k$  cutoff in the power spectrum.

Moreover, it can be deduced that the Poisson noise from lower-mass PBHs appears to result in a lower predicted abundance of UDMHs, making them less likely to fall within the parameter space excluded by observational constraints on PBHs. However, as the PBH mass increases, the predicted abundance of UDMHs also rises, increasingly overlapping with regions previously ruled out by observational data. This suggests that the Poisson noise effect from lower-mass PBHs supports SC dark matter scenarios, whereas the corresponding effect from higher-mass PBHs aligns with MC scenarios. Notably, these findings exhibit strong agreement with the PBH mass spectrum inferred from the thermal history of the early Universe.

### IV. CONCLUSIONS

In this work, we have studied the effect of Poisson noise from stellar-mass PBHs on the abundance of UDMHs. In this regard, we have demonstrated that incorporating Poisson noise into the matter power spectrum significantly alters the expected mass distribution of UDMHs. In particular, we have shown that the contribution of Poisson noise to struc-

ture formation is highly sensitive to the mass of PBHs, with larger masses leading to stronger modifications in the power spectrum. This effect ultimately influences the emergence and characteristics of UDMHs during the radiation-dominated era, distinguishing them from conventional dark matter structures.

We have analyzed a modified matter power spectrum and revealed that the Poisson fluctuations induced by PBHs create distinct enhancements in the small-scale regime. The magnitude of these enhancements depends on the PBH mass, leading to a nontrivial interplay between stochastic fluctuations and primordial density perturbations. We have provided quantitative evidence that the presence of lighter PBHs strengthens the SC dark matter scenario, while heavier PBHs favor the MC dark matter model. This result offers new insights into the nature of dark matter composition, as well as the potential observational signatures of PBHs as a dark matter candidate.

Furthermore, we have compared different halo mass functions, including the PS, ST, DP1, and DP2 formalisms, and examined the impact of incorporating more realistic mass functions in predicting the abundance of UDMHs. We have found that the inclusion of physical corrections, such as angular momentum and dynamical friction, significantly modifies the predicted UDMH abundance. The DP1 mass function, which accounts for angular momentum corrections, predicts a higher abundance of high-mass UDMHs compared to the other models. Conversely, the DP2 function, which incorporates dynamical friction effects, suppresses the formation of high-mass UDMHs. These findings emphasize the importance of including additional physical effects in analytical models of structure formation.

The observational implications of our findings are also noteworthy. The predicted abundance of UDMHs is closely tied to the mass spectrum of PBHs inferred from the thermal history of the early Universe. In the SC scenario, where PBHs constitute the entirety of dark matter, the clustering of smaller PBHs is expected to drive UDMH formation. In contrast, in the MC scenario, the formation of UDMHs is primarily influenced by the virialization of various dark matter components. Our results also suggest that Poisson noise from lighter PBHs predicts UDMHs whose abundance is likely to be constrained by current observational limits, while higher-mass PBHs lead to UDMH abundances that overlap with excluded parameter regions. This finding reinforces the role of UDMHs as a potential probe for constraining PBH models in future cosmological surveys.

Despite the robustness of our conclusions, several theoretical uncertainties may have impacted our results. These include potential modifications to the initial conditions of PBH formation, uncertainties in the power spectrum at small scales, and nonlinear effects that may alter the interplay between Poisson noise and large-scale structure formation. Future work should aim to refine these aspects by incorporating numerical simulations that capture the nonlinear evolution of PBH clustering and the subsequent formation of UDMHs. Additionally, improved constraints from upcoming gravitational wave observatories and high-redshift structure surveys will be instrumental in validating our predictions and further exploring the implications of Poisson noise in the context of dark matter structure formation.

- 
- [1] Y. B. Zeldovich, *MNRAS* **160**, 1P (1972).
- [2] A. A. Starobinsky, *Physics Letters B* **117**, 175 (1982).
- [3] A. H. Guth and S. Y. Pi, *Phys. Rev. Lett.* **49**, 1110 (1982).
- [4] H. Kodama and M. Sasaki, *Progress of Theoretical Physics Supplement* **78**, 1 (1984).
- [5] V. F. Mukhanov, H. A. Feldman, and R. H. Brandenberger, *Physics Reports* **215**, 203 (1992).
- [6] A. A. Starobinskij, *Soviet Journal of Experimental and Theoretical Physics Letters* **55**, 489 (1992).
- [7] D. J. H. Chung, E. W. Kolb, A. Riotto, and I. I. Tkachev, *Phys. Rev. D* **62**, 043508 (2000), [arXiv:hep-ph/9910437 \[hep-ph\]](#).
- [8] J. Martin and R. H. Brandenberger, *Phys. Rev. D* **63**, 123501 (2001), [arXiv:hep-th/0005209 \[hep-th\]](#).
- [9] M. Joy, V. Sahni, and A. A. Starobinsky, *Phys. Rev. D* **77**, 023514 (2008), [arXiv:0711.1585 \[astro-ph\]](#).
- [10] C. T. Byrnes and K.-Y. Choi, *Advances in Astronomy* **2010**, 724525 (2010), [arXiv:1002.3110 \[astro-ph.CO\]](#).
- [11] E. Komatsu, *Classical and Quantum Gravity* **27**, 124010 (2010), [arXiv:1003.6097 \[astro-ph.CO\]](#).
- [12] L. Ackerman, W. Fischler, S. Kundu, and N. Sivanandam, *JCAP* **2011**, 024 (2011), [arXiv:1007.3511 \[astro-ph.CO\]](#).
- [13] P. Villanueva-Domingo, O. Mena, and S. Palomares-Ruiz, *Front. Astron. Space Sci.* **8**, 87 (2021), [arXiv:2103.12087 \[astro-ph.CO\]](#).
- [14] A. M. Green and B. J. Kavanagh, *J. Phys. G Nucl. Part. Phys.* **48**, 043001 (2021), [arXiv:2007.10722 \[astro-ph.CO\]](#).
- [15] B. Carr and F. Kuhnel, [arXiv e-prints](#), [arXiv:2110.02821 \(2021\)](#), [arXiv:2110.02821 \[astro-ph.CO\]](#).
- [16] M. Korwar and S. Profumo, *J. Cosmol. Astropart. Phys* **2023**, 054 (2023), [arXiv:2302.04408 \[hep-ph\]](#).
- [17] S. Bird, I. Cholis, J. B. Muñoz, Y. Ali-Haïmoud, M. Kamionkowski, E. D. Kovetz, A. Raccanelli, and A. G. Riess, *Phys. Rev. Lett.* **116**, 201301 (2016), [arXiv:1603.00464 \[astro-ph.CO\]](#).
- [18] M. Sasaki, T. Suyama, T. Tanaka, and S. Yokoyama, *Phys. Rev. Lett.* **117**, 061101 (2016), [arXiv:1603.08338 \[astro-ph.CO\]](#).
- [19] S. Fakhry, J. T. Firouzjaee, and M. Farhoudi, *Phys. Rev. D* **103**, 123014 (2021), [arXiv:2012.03211 \[astro-ph.CO\]](#).
- [20] S. Fakhry, M. Naseri, J. T. Firouzjaee, and M. Farhoudi, *Phys. Rev. D* **105**, 043525 (2022), [arXiv:2106.06265 \[astro-ph.CO\]](#).
- [21] S. Fakhry, Z. Salehnia, A. Shirmohammadi, and J. T. Firouzjaee, *APJ* **941**, 36 (2022), [arXiv:2209.08909 \[astro-ph.CO\]](#).
- [22] S. Fakhry, S. S. Tabasi, and J. T. Firouzjaee, *Phys. Dark Universe* **41**, 101244 (2023), [arXiv:2210.13558 \[astro-ph.CO\]](#).
- [23] S. Fakhry and A. Del Popolo, *Phys. Rev. D* **107**, 063507 (2023), [arXiv:2212.08646 \[astro-ph.CO\]](#).
- [24] S. Fakhry, Z. Salehnia, A. Shirmohammadi, M. G. Yengejeh, and J. T. Firouzjaee, *APJ* **947**, 46 (2023), [arXiv:2301.02349 \[astro-ph.CO\]](#).
- [25] S. Fakhry, *ApJ* **961**, 8 (2024), [arXiv:2308.11049 \[gr-qc\]](#).
- [26] S. Fakhry, M. Shiravand, and M. Farhang, *ApJ* **966**, 235 (2024), [arXiv:2401.15171 \[gr-qc\]](#).

- [27] S. Fakhry, S. Gholamhoseinian, and M. Farhang, *ApJ* **976**, 248 (2024), arXiv:2408.11995 [gr-qc].
- [28] N. Afshordi, P. McDonald, and D. N. Spergel, *ApJL* **594**, L71 (2003), arXiv:astro-ph/0302035 [astro-ph].
- [29] S. Andrés Vallejo-Peña and A. Enea Romano, *JCAP* **2019**, 015 (2019), arXiv:1904.07503 [astro-ph.CO].
- [30] O. Özsoy, S. Parameswaran, G. Tasinato, and I. Zavala, *JCAP* **2018**, 005 (2018), arXiv:1803.07626 [hep-th].
- [31] Q. Wang, Y.-C. Liu, B.-Y. Su, and N. Li, arXiv e-prints, arXiv:2111.10028 (2021), arXiv:2111.10028 [astro-ph.CO].
- [32] J. García-Bellido and E. Ruiz Morales, *Physics of the Dark Universe* **18**, 47 (2017), arXiv:1702.03901 [astro-ph.CO].
- [33] D. Huterer and et al., *Astroparticle Physics* **63**, 23 (2015), arXiv:1309.5385 [astro-ph.CO].
- [34] G.-W. Yuan, L. Lei, Y.-Z. Wang, B. Wang, Y.-Y. Wang, C. Chen, Z.-Q. Shen, Y.-F. Cai, and Y.-Z. Fan, *Science China Physics, Mechanics, and Astronomy* **67**, 109512 (2024), arXiv:2303.09391 [astro-ph.CO].
- [35] H.-L. Huang, J.-Q. Jiang, and Y.-S. Piao, *Phys. Rev. D* **110**, 103540 (2024), arXiv:2407.15781 [astro-ph.CO].
- [36] P. Scott and S. Sivertsson, *Phys. Rev. Lett.* **103**, 211301 (2009), arXiv:0908.4082 [astro-ph.CO].
- [37] M. Ricotti and A. Gould, *APJ* **707**, 979 (2009), arXiv:0908.0735 [astro-ph.CO].
- [38] M. S. Delos and J. Silk, *MNRAS* **520**, 4370 (2023), arXiv:2210.04904 [astro-ph.CO].
- [39] S. Fakhry, M. Farhang, and A. Del Popolo, *Physics of the Dark Universe* **46**, 101544 (2024), arXiv:2311.15307 [astro-ph.CO].
- [40] T. Bringmann, P. Scott, and Y. Akrami, *Phys. Rev. D* **85**, 125027 (2012), arXiv:1110.2484 [astro-ph.CO].
- [41] M. Gosenca, J. Adamek, C. T. Byrnes, and S. Hotchkiss, *Phys. Rev. D* **96**, 123519 (2017), arXiv:1710.02055 [astro-ph.CO].
- [42] M. S. Delos, A. L. Erickcek, A. P. Bailey, and M. A. Alvarez, *Phys. Rev. D* **98**, 063527 (2018), arXiv:1806.07389 [astro-ph.CO].
- [43] S. D. M. White, *MNRAS* **517**, L46 (2022), arXiv:2207.13565 [astro-ph.CO].
- [44] A. Del Popolo and S. Fakhry, *Phys. Dark Universe* **41**, 101259 (2023), arXiv:2305.19817 [astro-ph.CO].
- [45] A. Del Popolo and S. Fakhry, *Astronomy Reports* **68**, 19 (2024).
- [46] E. W. Kolb and I. I. Tkachev, *Phys. Rev. D* **50**, 769 (1994), arXiv:astro-ph/9403011 [astro-ph].
- [47] V. I. Dokuchaev and Y. N. Eroshenko, *Sov. J. Exp. Theor. Phys.* **94**, 1 (2002), arXiv:astro-ph/0202021 [astro-ph].
- [48] V. Berezhinsky, V. Dokuchaev, Y. Eroshenko, M. Kachelrieß, and M. A. Solberg, *Phys. Rev. D* **81**, 103529 (2010), arXiv:1002.3444 [astro-ph.CO].
- [49] V. S. Berezhinsky, V. I. Dokuchaev, and Y. N. Eroshenko, *J. Cosmol. Astropart. Phys* **2013**, 059 (2013), arXiv:1308.6742 [astro-ph.CO].
- [50] T. Nakama, K. Kohri, and J. Silk, *Phys. Rev. D* **99**, 123530 (2019), arXiv:1905.04477 [astro-ph.CO].
- [51] W. Hu and N. Sugiyama, *APJ* **471**, 542 (1996), arXiv:astro-ph/9510117 [astro-ph].
- [52] R. K. Sheth, H. J. Mo, and G. Tormen, *MNRAS* **323**, 1 (2001), arXiv:astro-ph/9907024 [astro-ph].
- [53] J. R. Bond, S. Cole, G. Efstathiou, and N. Kaiser, *APJ* **379**, 440 (1991).
- [54] C. Blanco, M. S. Delos, A. L. Erickcek, and D. Hooper, *Phys. Rev. D* **100**, 103010 (2019), arXiv:1906.00010 [astro-ph.CO].
- [55] C. Lacey and S. Cole, *MNRAS* **271**, 676 (1994), arXiv:astro-ph/9402069 [astro-ph].
- [56] R. K. Sheth, *MNRAS* **300**, 1057 (1998), arXiv:astro-ph/9805319 [astro-ph].
- [57] R. K. Sheth and G. Tormen, *MNRAS* **329**, 61 (2002), arXiv:astro-ph/0105113 [astro-ph].
- [58] A. R. Zentner, *Int. J. Mod. Phys. D* **16**, 763 (2007), arXiv:astro-ph/0611454 [astro-ph].
- [59] A. Del Popolo, F. Pace, and M. Le Delliou, *J. Cosmol. Astropart. Phys* **2017**, 032 (2017), arXiv:1703.06918 [astro-ph.CO].
- [60] A. Del Popolo, *APJ* **637**, 12 (2006), arXiv:astro-ph/0609100 [astro-ph].
- [61] R. Bean and J. Magueijo, *Phys. Rev. D* **66**, 063505 (2002), arXiv:astro-ph/0204486 [astro-ph].
- [62] Planck Collaboration, N. Aghanim, and et al., *AAP* **641**, A6 (2020), arXiv:1807.06209 [astro-ph.CO].
- [63] B. Carr, S. Clesse, J. Garcia-Bellido, and F. Kuhnel, arXiv e-prints, arXiv:1906.08217 (2019), arXiv:1906.08217 [astro-ph.CO].
- [64] P. Tisserand, et al., and EROS-2 Collaboration, *AAP* **469**, 387 (2007), arXiv:astro-ph/0607207 [astro-ph].
- [65] T. D. Brandt, *APJL* **824**, L31 (2016), arXiv:1605.03665 [astro-ph.GA].
- [66] S. Jung and C. S. Shin, *Phys. Rev. Lett.* **122**, 041103 (2019), arXiv:1712.01396 [astro-ph.CO].
- [67] H. Niikura, M. Takada, S. Yokoyama, T. Sumi, and S. Masaki, *Phys. Rev. D* **99**, 083503 (2019), arXiv:1901.07120 [astro-ph.CO].
- [68] Z.-C. Chen and Q.-G. Huang, *J. Cosmol. Astropart. Phys* **2020**, 039 (2020), arXiv:1904.02396 [astro-ph.CO].
- [69] B. P. e. a. Abbott, LIGO Scientific Collaboration, and Virgo Collaboration, *Phys. Rev. D* **100**, 024017 (2019), arXiv:1904.08976 [astro-ph.CO].
- [70] R. e. a. Abbott, LIGO Scientific Collaboration, and Virgo Collaboration, *Phys. Rev. Lett.* **129**, 061104 (2022), arXiv:2109.12197 [astro-ph.CO].
- [71] B. Carr, M. Raidal, T. Tenkanen, V. Vaskonen, and H. Veermäe, *Phys. Rev. D* **96**, 023514 (2017), arXiv:1705.05567 [astro-ph.CO].
- [72] K. Kohri, T. Nakama, and T. Suyama, *Phys. Rev. D* **90**, 083514 (2014), arXiv:1405.5999 [astro-ph.CO].